Nuclear Materials Authority
P.O.Box 530 Maadi, Cairo, Egypt

ISSN 2314-5609
Nuclear Sciences Scientific Journal
6, 1-16
2017
http://www.ssnma.com

GEOLOGY, GEOCHEMISTRY AND RADIOACTIVITY OF DYKE SWARMS AT WADI EL AKHDAR AREA, SOUTHCENTRAL SINAI, EGYPT

ABDEL MOEZ A. SADEK and ABDEL HADI A. ABBAS
Nuclear Materials Authority, P.O. 530, Maadi, Cairo, Egypt.

ABSTRACT

Wadi El Akhdar area is dissected by two main dyke trends cutting mainly the older granites. The oldest dykes trend NE-SW comprising swarms of nearly parallel basic dykes (basalt). The intermediate dykes trending NW-SE (basaltic-andesite and trachy-andesite) cut the former dyke trend. The major dykes trending NE-SW are acidic (rhyolite and granophyre) representing the terminate emplacement of the studied dykes. The rocks of the dyke swarms were derived from high K-calc-alkaline magma and subjected to fractional crystallization. They are of hyperaluminous in nature and were erupted in within-plate tectonic and volcanic arc granitoid environments. In the studied dykes, Rb/Sr ratio for the basic and intermediate members are far <0.7 indicating direct derivation from the upper mantle; while acidic ones with Rb/Sr ratio up to 10.7 values suggest the presence of felsic materials in their source and were derived from sialic crust or affected by crustal contamination.

The field radiometric survey and laboratory radiometric measurements indicate that the rhyolite and granophyre dykes are the most important from the radioactive point of view. They are characterized by the presence of uranium and thorium minerals, together with some rare metal minerals. The radioactive minerals are lithologically controlled due to post magmatic processes which cause addition of uranium. Uranophane, uranothorite, columbite, zircon and monazite are the main radioactive minerals in the examined acidic dykes.

INTRODUCTION

The older and younger granites of Wadi El Akhdar area are intruded by a large number of post granite dykes; which form one of the dyke swarms recorded in south central Sinai (Fig.1). These dykes were subdivided petrographically by Zalata (1988) into acidic (granophyric quartz-feldspar porphyry, quartz-feldspar porphyry and fine-grained biotite granite), intermediate and basic (andesite, andesite porphyry and dolerite), alkaline and lamprophyre (bostonite, trachyte, and spessartite) and filled by ferruginous quartz arenite. Ahmed and Youssef (1976) on their study of airphoto interpretation of dyke swarms in the area around Feiran Oasis concluded that nearly all dykes trend in the NE-SW direction except two long olivine dolerite dykes which have WNW-ESE trend.

Friz (1987) studied the dyke rocks at Wadi el Sheikh area, located at the southern border of Wadi El Akhdar area. He distinguished two groups of dyke rocks as a)The older group, trending N 20°-35° E, is intermediate in composition and displays calc-alkaline character of subduction-related rocks in active continental margins. b)The younger group, which trends N 40°– 55 W, is mildly alkaline within-

plate basalts. El Mowafy (2008) studied the dyke rocks at Gabal Minadier area southcentral Sinai. He concluded that in Gabal Minadier area the dyke swarms are composed of rhyolite, andesite and basaltic-andesite. The rhyolite dykes are the dominant set and mainly oriented in NE, the andesite dykes represent the terminate emplacement of the dyke intrusion at Gabal Minadier area whereas the basaltic-andesite dykes intrude all the basement rock units of the studied area and trend mainly NNW, NW and NE.

The present study is an attempt to throw light on the petrogenesis and radioactivity of the dyke swarms recorded in Wadi El Akhdar area southcentral Sinai Egypt.

GEOLOGIC SETTING

Wadi El Akhdar area is located between lat. 28° 48' 45" and 28°54' 30" N and long. 33º 33' 41" and 33° 35' 9"E in the Southcentral Sinai, Egypt (Fig.1). The basement rocks of Wadi El Akhdar area are represented by younger and older granitoids composing about 75% of the mapped area. The older granites are mainly tonalite and granodiorite and constitute the largest part of the mapped area; whereas the younger granite is less abundant and are represented by monzogranite of Gabal Hamra pluton cropping out at the northwestern part of the studied area. They are dissected by dyke swarms having NE-SW and NW-SE trends. These dyke swarms posses sharp contacts and child margins with their country rocks. The well developed slickensides observed along the dyke sides suggest that these dykes were invaded along active shear planes. They form moderately to low elevated outcrops steeply inclined (67º-79º). They usually range from 1 to 25 m in width and from1 to 10 km in length (Fig.2). The thick dykes usually show a pronounced grain size variation increasing from margin to center.

The chronological sequence of the studied dykes is arranged on the basis of cross cutting relationships. They were intruded at different periods as the basic dykes then acidic dykes and both of them invaded by the intermediate dykes (Fig.3a&b).

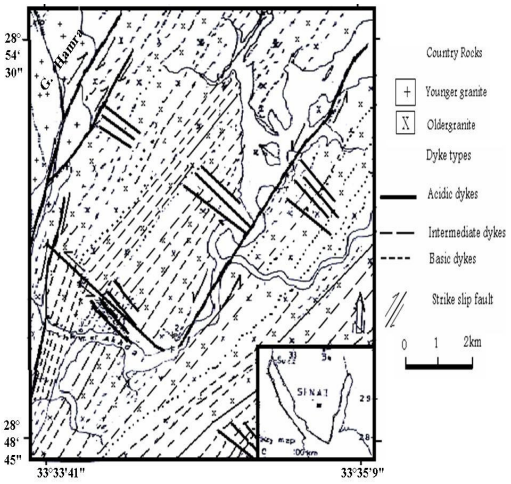

Fig. 1: Geological map of Wadi El Akhdar area, Southcentral Sinai, Egypt (Modified after Zalata, 1988)

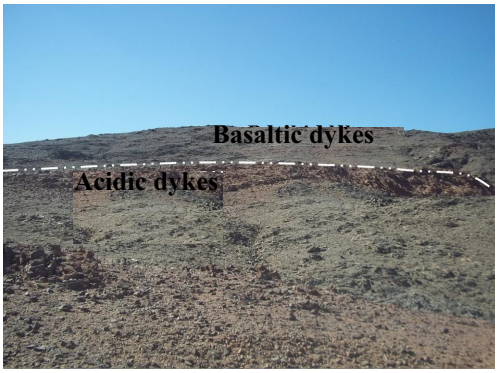

Fig.2: Photographs showing dyke swarms cutting Wadi El Akhdar area

PETROGRAPHY

The studied dyke swarms are of three main types namely acidic, intermediate and basic dykes. The acidic dykes are represented mainly by rhyolite and granophyre. The intermediate dykes comprise trachyte and trachy-andesite. While the basic dykes are represented by basalt and basaltic-andesite.

Fig. 3 a&b : Google earth view showing dyke swarms at Wadi El Akhdar area

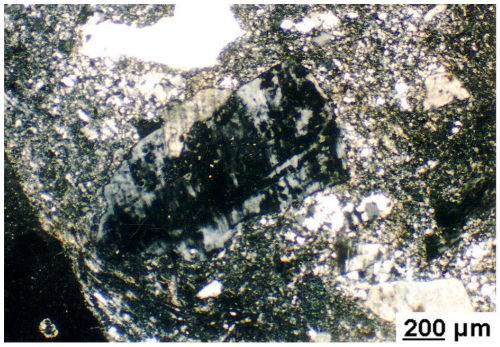

Fig.4: Phenocrysts of perthite occur as cumulophyric aggregates in rhyolite dyke

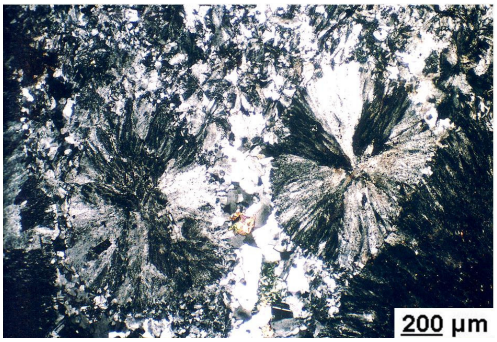

Fig. 5: Spherulitic texture in rhyolite dykes

Acidic Dykes

Rhyolite dykes

Rhyolite dykes are fine-grained with variable amounts of phenocrysts (10-35 vol. %). The phenocrysts occur either as discrete crystals or as glomerophyric or cumulophyric aggregates (Fig.4). They are represented by abundant K-feldspar and quartz together with fair amounts of albite, opaques and accessories. The phenocrysts are set in a microcrystalline groundmass showing various textures, including micrographic, porphyritic and spherultic textures (Fig.5). Micrographic intergrowth between K-feldspar and quartz surrounds the porphyritic quartz crystals. The K-feldspar crystals are lath-shaped of orthoclase and reach 3.5 mm in length and 2.0 mm in width. They usually show simple twinning and are slightly altered. Quartz occurs as subhedral phenocrysts, 0.7 to 3.4 mm across. Sometimes quartz phenocrysts are corroded showing rounded corners and embayments filled by the groundmass.

Granophyre dykes

Granophyre dykes are porphyritic and the phenocrysts (15-45 vol. %) may reach 4.0 mm in length. They are mainly composed of K-feldspar, albite, quartz and biotite. These phenocrysts are set in a microcrystalline felsic groundmass exhibiting granophyric and micrographic textures (Fig. 6). The K-feldspar phenocrysts form anhedral to subhedral crystals usually showing simple twinning. The albite phenocrysts are mostly clear and show fine lamellar twinning. Sometimes, few albite crystals are corroded and embayed by the groundmass. Quartz is present in the form of individual, commonly porphyritic crystals or

Fig. 6: Granophyric and micrographic textures in granophyre dykes

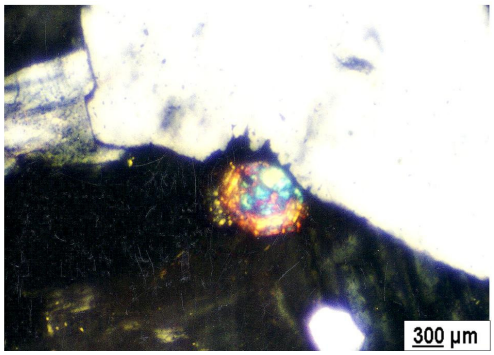

Fig. 7: Zircon occurs as inclusions in feldspar trachyte dykes

intergrown with K-feldspar developing granophyric and micrographic textures. Biotite occurs as small anhedral phenocrysts that are marginally altered to fibrous chlorite or as fine flakes in the groundmass.

Intermediate Dykes

Trachyte dykes

Trachyte dykes are fine-grained consisting of feldspars and interstitial sodic pyroxenes exhibiting marked flow texture. Biotite is minor constituent. Opaques, apatite and zircon are accessory minerals; whereas the secondary minerals include chlorite, quartz and carbonates. Feldspar laths are the most abundant constituents and form about 70% of the rock. They are mainly albite with subordinate sanidine. Pyroxenes are represented by aegirine occurring as fine prismatic crystals between the feldspar laths. Biotite crystals are sporadically scattered in the rock. They are characterized by a deep reddish brown color and strong pleochroism. Apatite occurs as short stumpy prisms which contain abundant dusty inclusions. Zircon occurs as inclusions in feldspar laths (Fig. 7). Secondary carbonates are found whereas secondary quartz occurs as fine granular aggregates in the ground mass.

Trachy-andesite dykes

The trachyandesite dykes are massive fine-grained and dark gray in color. They are mainly composed of plagioclase, quartz, sanidine, biotite and hornblende. Accessory minerals are rutile and iron oxides. Plagioclase forms euhedral laths of andesine composition, commonly altered to epidote and zoisite. Sanidine is present as subhedral tabular crystals. Quartz occurs as anhedral crystals that fill the interstitial spaces between the feldspar crystals. Biotite forms irregular flakes.

Basic Dykes

The basalt and basaltic-andesite dykes are the most common rock varieties among the mafic dyke swarms. They are mainly massive and the color varies from black to grayish green according to the extent degree of alteration.

Basaltic dykes

Microscopically they are consisting essentially of plagioclase, augite and subordinate amount of olivine. Apatite and sphene are accessory minerals whereas biotite and calcite are secondary minerals. ***Plagioclase*** $_{(An\ 35)}$ occur either as subhedral tabular phenocryst of plagioclase crystals set in fine-grained groundmass composed of plagioclase laths (Fig.8). In some places plagioclase shows alteration to saussurite. ***Olivine*** occurs as oval crystals characterized by mesh texture partail-

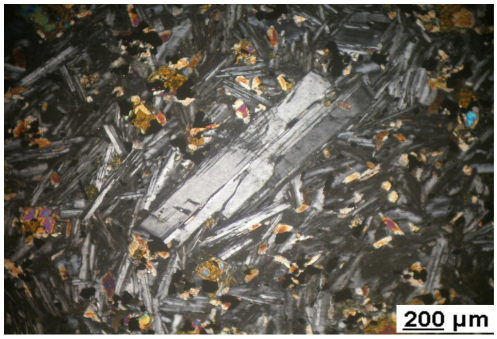

Fig. 8: Phenocryst of plagioclase in fine-grained groundmass in Basaltic dykes

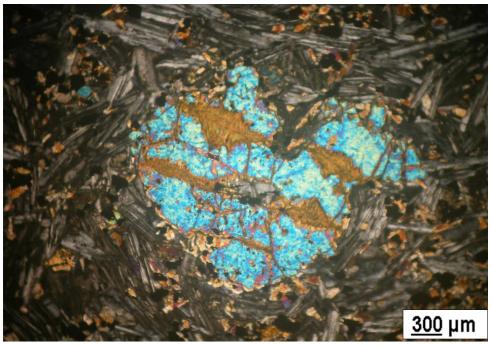

Fig.9: Olivine partially altered to biotite along the fractures in basaltic dykes

ly altered to biotite along the fractures (Fig.9). ***Augite*** occurs in the form of pseudomorph of olivine and granular aggregates in the groundmass partly altered to chlorite. ***Apatite*** forms minute prismatic crystals, with six sided cross sections generally enclosed in essential minerals. Sphene occurs as rhombic grains within augite crystals.

Basaltic-andesite dykes

They are composed essentially of phenocrysts of plagioclase, augite and hornblende set in a fine-grained groundmass consisting of plagioclase, augite and hornblende. Accessory minerals are apatite, sphene and opaques. ***Plagioclase*** is mainly andesine to labraodorite, occurring as subhedral crystals commonly twinned and zoned with marked epidote and zoisite aggregates. ***Augite*** is present as subhedral prismatic crystals and moderately altered to actinolite and/or chlorite. ***Hornblende*** usually forms euhedral crystals with perfect six-sided outlines.

GEOCHEMISTRY

The chemical analyses of thirty dyke samples for major oxides and some trace elements were carried out using a PW 1404 XRF spectrometer following the procedures of Philips (1994) for correction of matrix. These instruments are hosted in the mineralogical Institute, Trieste University, Italy. The analyses of different studied dykes in Wadi El Akhdar area are shown in Tables (1, 2 &3).

Geochemical Classification

The classification of the studied dykes was geochemically confirmed by plotting the analyses on the TAS diagram (Fig.10), recommended by the IUGS (Le Maitre et al. 1989). It shows that the analyzed samples fall in the fields of basalt, basaltic-andesite, trachy-andesite, trachyte and rhyolite. The granophyre samples plot in the rhyolite field. They are mainly sub-alkaline to alkaline rocks.

Chemical Characteristics, Magma Type and Tectonic Setting

Chemical variations within rocks of one or more magma series of different regions may be visualized by applying Harker diagrams. The major element variations relative to SiO_2 are used as an index of differentiation for the studied dykes (Figs.11-14). The oxides FeO^t, MgO, CaO and Al_2O_3 decrease regularly from basalt to basaltic-andesite, trachy-andesite and trachyte to rhyolite with increasing SiO_2. On contrast, K_2O and Na_2O show a continuous increase with increasing SiO_2(Figs. 15&16). The curvlinear systematic variations for most of the major oxides in the studied dykes could be interpreted as evidence of fractional crystallization.

Table 1: Major oxides (wt %) and some trace elements (ppm) of the studied basic dykes

Rock Samples	Basic dykes							
	Basalt				Basaltic-andesite			
	1	2	3	4	5	6	7	8
SiO_2	46. 39	52.03	47.40	47.11	54.06	54. 65	54. 65	56.14
TiO_2	3.30	1.78	3.15	3.04	1.07	1.25	1.18	1.77
Al_2O_3	17.13	15.89	14.02	14.05	14.16	16.38	16.90	14.59
FeOt	11.31	8.85	13.56	14.20	8.57	8.29	7.75	9.15
MnO	0.43	0.13	0.18	0.19	0.15	0.14	0.12	0.15
MgO	5.43	6.36	7.24	9.05	8.63	5.04	4.11	3.42
CaO	7.20	7.45	7.30	5.51	7. 40	7.24	7.51	6.22
Na_2O	3.63	3.51	2.44	2.80	2.59	3.41	3.46	3.36
K_2O	2.40	1.11	1.59	1.31	1.15	1.42	1.89	2.20
P_2O_5	0.64	0.77	0.86	0.44	0.26	0.39	0.39	0.54
L.O.I.	1.96	1.93	2.13	1.86	1.76	1.36	1.62	2.13
Total	99.82	99.81	99.87	99.56	99.80	99.57	99.58	99.67
Trace elements (ppm)								
Ba	797	463	540	491	767	410	463	606
Rb	41	55	36	31	60	60	55	58
Nb	83	7	30	34	5	6	7	10
Zr	129	139	129	116	142	87	124	90
Sr	499	680	628	605	560	661	680	549
Y	41	27	45	40	26	25	27	40
Cr	152	59	30	26	412	66	59	9
Ni	143	39	53	34	107	15	39	15
La	63	21	45	37	22	21	21	29
Ce	94	38	85	65	29	39	38	63
Nd	48	23	50	35	19	19	23	38
Some geochemical ratios								
Na_2O/K_2O	1.51	3.16	1.53	2.14	2.25	2.40	1.83	1.53
Rb/Sr	0.08	0.08	0.06	0.05	0.11	0.09	0.08	0.11
Ba/Rb	19.44	8.42	15.00	15.84	12.78	6.83	8.42	10.45
Y/Nb	0.49	3.86	1.50	1.18	5.20	4.17	3.86	4.00
Zr/Sr	0.26	0.20	0.20	0.19	0.25	0.13	0.18	0.16

Table 3: Major oxides (wt %) and some trace elements (ppm) of the studied acidic dykes

Rock Samples	Acidic dykes							
	Rhyolite				Granophyre			
	23	24	25	26	27	28	29	30
SiO_2	76. 15	70.39	76.14	73.45	74.21	75.49	74. 87	74.45
TiO_2	0.02	0.31	0.03	0.20	0.17	0.06	0.03	0.05
Al_2O_3	12.60	14.77	12.56	13.45	13.35	13.00	12.81	13.50
FeOt	1.03	2.21	1 .36	1 .44	1.25	1.12	1.50	0.72
MnO	0.01	0.06	0.01	0.04	0.03	0.02	0.01	0.03
MgO	0.06	1.06	0.04	0.29	0.25	0.12	0.03	0.08
CaO	0.15	1.70	0.12	1.16	0. 73	0.25	0.33	0.42
Na_2O	5.45	4.74	5.64	4.38	4.48	4.52	5.58	4.16
K_2O	3.25	3.36	2. 95	4.45	4.41	4.39	3.60	4.30
P_2O_5	0.02	0.13	0.01	0.06	0.05	0.01	0.01	0.01
L.O.I.	0.91	0.83	0.77	0.69	0.68	0.53	0.71	0.91
Total	99.65	99.56	99.63	99.61	99.61	99.51	99.48	98.63
Trace elements (ppm)								
Ba	52	723	119	717	578	70	66	27
Rb	281	179	232	299	150	143	182	149
Nb	31	7	65	11	29	22	72	19
Zr	657	967	780	879	635	256	602	287
Sr	37	320	31	174	135	35	21	28
Y	62	15	59	23	21	73	76	75
Cr	6	7	5	6	8	11	7	7
Ni	1	2	1	1	2	2	1	1
La	31	32	9	50	48	12	12	11
Ce	26	51	14	81	73	16	18	27
Nd	54	20	14	34	32	17	28	21
Some geochemical ratios								
Na_2O/K_2O	1.68	1.41	1.91	0.98	1.02	1.03	1.55	0.97
Rb/Sr	7.59	0.56	7.48	1.72	1.11	4.09	8.67	5.32
Ba/Rb	0.19	4.04	0.51	2.40	3.85	0.49	0.36	0.18
Y/Nb	2.00	2.14	0.91	2.09	0.72	3.32	1.06	3.95
Zr/Sr	17.76	3.02	25.16	5.05	4.70	7.31	28.67	10.25

Table 2: Major oxides (wt %) and some trace elements (ppm) of the studied intermediate dykes

Rock Samples	Intermediate dykes													
	Trachy-andesite								Trachyte					
	9	10	11	12	13	14	15	16	17	18	19	20	21	22
SiO_2	57.02	57.88	58.48	55.52	58.80	57.62	60.03	54.60	63.44	67.33	63.91	64.62	67.32	63. 14
TiO_2	1.39	1.41	1.55	1. 61	1.42	1.70	0.58	1.73	0.99	0.71	1.17	1.11	1.02	1.00
Al_2O_3	14.81	15.41	15.16	14.29	15.64	14.33	15.40	14.06	14.86	14.84	13.80	14.03	13.33	14.95
FeO^t	9.35	7.75	8.29	11.05	7.60	8.71	8.01	11.75	6.12	4.17	6.03	5.93	5.18	6.13
MnO	0.23	0.11	0.12	0.21	0.10	0.15	0.19	0.23	0.11	0.12	0.19	0.23	0.17	0.10
MgO	3.40	3.22	2.88	2.50	2.93	2.96	0.32	4.11	1.42	1.07	1.80	1.87	1.74	2.03
CaO	3.49	5.49	4.73	4.62	5.03	5.14	4.91	3.67	3.21	0.51	2.70	1.99	1.96	3.65
Na_2O	3.93	3.70	3.54	3.91	3.52	3.71	3.16	3.41	4.17	4.58	3.46	3.86	4.06	3.92
K_2O	3.29	2.86	2.61	3.24	2.78	3.18	5.45	3.37	3.49	5.16	4.68	4.14	3.44	2.87
P_2O_5	1.02	0.51	0.57	1.01	0.55	0.55	0.07	1.12	0.42	0.24	0.67	0.58	0.54	0.42
L.O.I.	1.65	1.41	1.86	1.59	1.29	1.71	1.57	1.60	1.56	1.06	1.21	1.31	0.89	1.47
Total	99.6	99.8	99.8	99.6	99.7	99.8	99.7	99.7	99.8	99.8	99.6	99.7	99.7	99.7
Trace elements (ppm)														
Ba	792	726	292	1067	722	793	337	1156	896	463	540	1737	1632	766
Rb	72	91	77	71	79	88	189	81	105	55	36	121	118	78
Nb	55	39	20	63	39	21	60	63	21	27	30	36	33	38
Zr	257	161	129	222	218	143	287	152	262	147	332	212	236	215
Sr	403	604	453	566	515	521	162	539	369	680	628	259	433	452
Y	70	46	38	74	47	43	84	73	39	27	45	90	83	47
Cr	13	26	29	6	25	22	12	11	8	59	30	9	12	4
Ni	1	25	15	3	18	21	2	6	3	39	53	2	1	4
La	34	38	41	91	35	41	113	88	96	21	45	118	106	36
Ce	55	59	77	173	73	81	214	176	158	38	85	221	202	63
Nd	23	37	41	99	42	45	131	97	114	23	50	134	125	37
Some geochemical ratios														
Na_2O/K_2O	1.19	1.29	1.36	1.21	1.27	1.17	0.58	1.01	1.19	0.89	0.74	0.93	1.18	1.37
Rb/Sr	0.18	0.15	0.17	0.13	0.15	0.17	1.17	0.15	0.28	0.08	0.06	0.47	0.27	0.17
Ba/Rb	11.0	7.98	3.79	15.03	9.14	9.01	1.78	14.27	8.53	8.42	15.00	14.36	13.83	9.82
Y/Nb	1.27	1.17	1.90	1.17	1.21	2.05	1.40	1.16	1.86	1.0	1.50	2.50	2.52	1.24
Zr/Sr	0.64	0.40	0.28	0.39	0.42	0.27	1.77	0.28	0.71	0.22	0.52	0.83	0.55	0.48

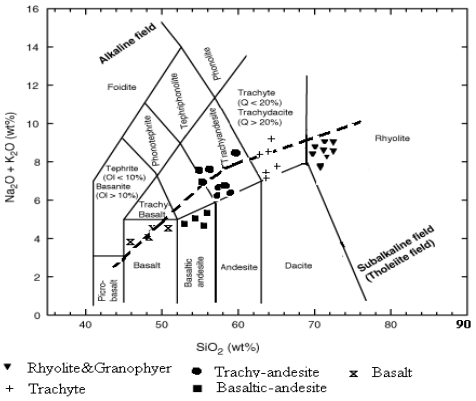

Fig. 10: Total alkali-silica (TAS) diagram for the studied volcanic rocks (According to Le Maitre et al., 1989). The plot displays the Irvine and Baragar (1971) alkaline/subalkaline division line (dashed line)

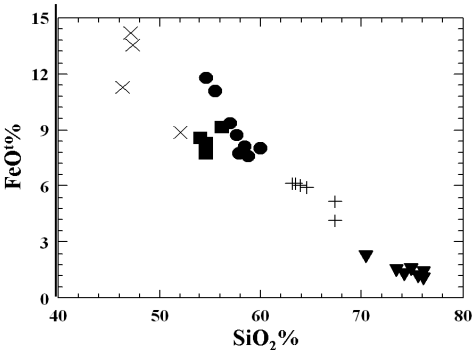

Fig. 11: Harker variation diagram of SiO_2 vs FeO% ,Symbols as in Fig.10

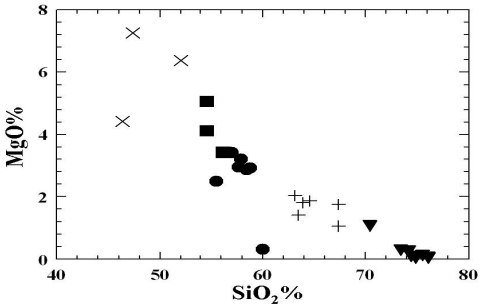

Fig. 12: Harker variation diagram of SiO_2 vs MgO%, Symbols as in Fig.10

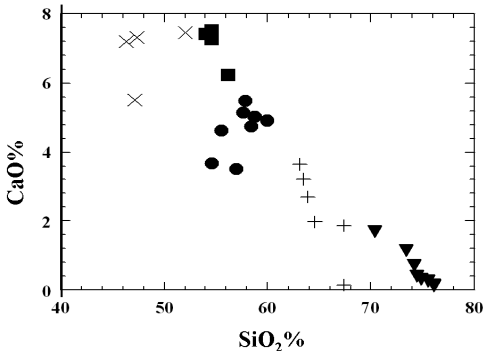

Fig. 13: Harker variation diagram of SiO_2 vs CaO%, Symbols as in Fig.10

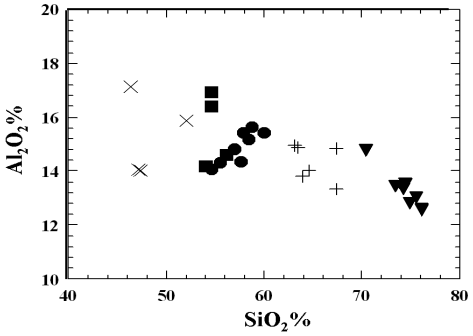

Fig. 14: Harker variation diagram of SiO_2 vs Al_2O_2%, Symbols as in Fig.10.

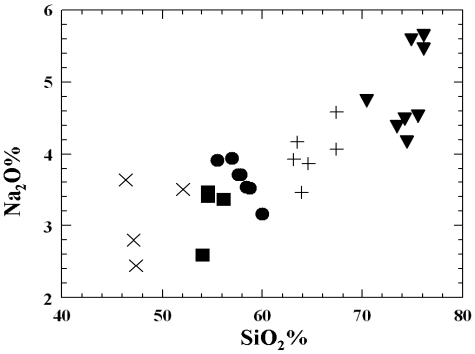

Fig. 15: Harker variation diagram of SiO_2 vs Na_2O%, Symbols as in Fig.10

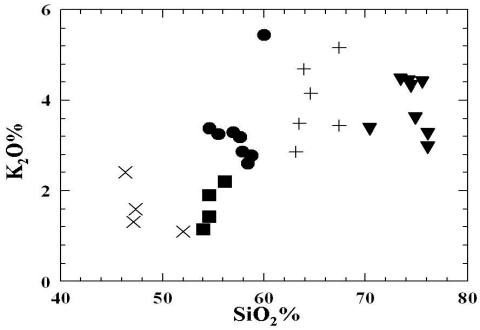

Fig. 16: Harker variation diagram of SiO_2 vs K_2O%, Symbols as in Fig.10.

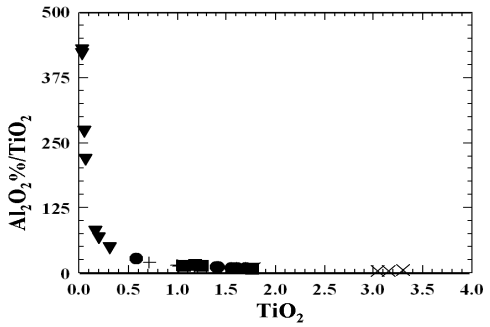

Fig. 17: Al_2O_3/TiO_2 Vs. TiO_2 binary diagram of the studied dykes (After Sun and Nesbitt. 1978). Symbols as in Fig.10

The Al_2O_3/TiO_2 versus TiO_2 binary diagram (After Sun and Nesbitt, 1978) reveals a complete spectrum of the studied dykes composition which may indicate continuous differentiation. Slight chemical gap is recorded at Al_2O_3/TiO_2 ratios of 48-26 between rhyolite and both of trachyte and trachy-andesite (Fig.17). On this diagram a clear distinction between the acidic dykes and the other groups is recorded. In the former group we notice a strong variation in the Al_2O_3/TiO_2 ratio within a very low and limited range of TiO_2. On the contrary, TiO_2 increases within a low and limited range of Al_2O_3 in the basic and intermediate groups.

The studied dykes pertain range from calc-alkaline to shoshonite nature (Fig.18) as shown on the K_2O-SiO_2 diagram proposed by Peccerillo & Taylor (1976) and modified by the IUGS (Le Maître et al, 1989).

The Na_2O+K_2O Vs. SiO_2 diagram of Iriven and Baragar, (1971), the majority of the studied dykes showing subalkaline magma type (Fig.19). The Zr/Y Vs. Zr digram of Pearse and Norry, (1979) showing the majority of the studied dykes to be of Within-plate tectonic setting with some samples plot in island arc tectonic setting (Fig. 20).

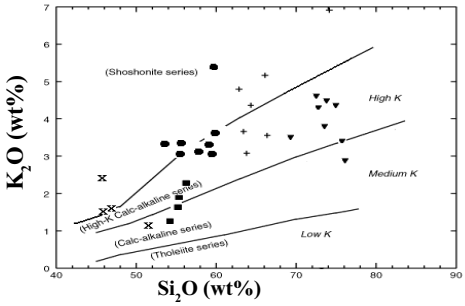

Fig. 18: SiO_2% Vs. K_2O% diagram (Peccerillo and Taylor, 1976) for the studied dykes.Lines separate between low K tholeiite, medium k calc-alkaline, high K calc-alkaline and shoshonite fields According to Le Maître et al., (1989). Symbols as in Fig.9

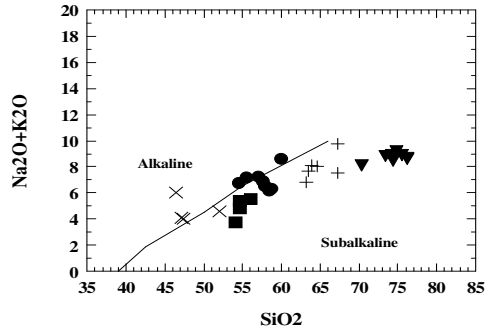

Fig.19: Na_2O+K_2O Vs. SiO_2 for the studied dykes (According to Iriven and Baragar, 1971) symbols as in Fig.10

PETROGENESIS

The Harker variation diagrams (Figs.11-13) show the regular decrease of Feo^t; MgO;

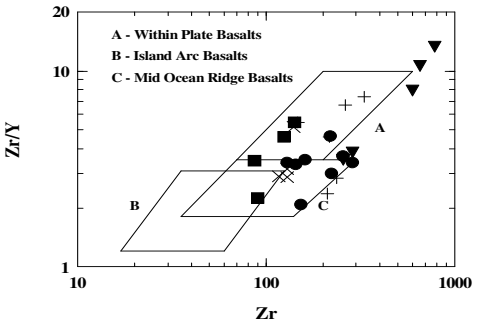

Fig. 20: Zr/Y Vs. Zr variation digram for, tectonic setting of the studied dykes (According to Pearce, J.A., and Norry, M.J., 1979). symbols as in Fig.10

and CaO. Accompanied by the regular increase in Na_2O and K_2O (Figs.15&16); from basalts to rhyolites, passing by the intermediate dykes, indicates in the major role of fractional crystallization in the origination of these dykes. However additional processes (namely metasomatism) by hydrothermal alkaline- rich solutions, clearly affecting the trachytes and rhyolites, cannot be neglected.

On the Al_2O_3/TiO_2 versus TiO_2 binary diagram (after Sun and Nesbitt, 1978), a clear distinction between the trend of evolution of the acidic dykes and the other groups (namely basic and intermediate) can be traced. In the former group we notice a strong variation in The Al_2O_3/TiO_2 ratio within a very low and limited range of TiO_2. On the contrary in the basic and intermediate group, TiO_2 increased within a very limited range of Al_2O_3 variation.

Bucanan (1982) suggested that the high Rb/Sr ratio (>1.5) indicates pre-existing felsic material in the source region of rocks, but low Rb/Sr ratio (<0.7) suggests derivation from the upper mantle. In the studied dykes, Rb/Sr ratio for the basic and intermediate members are far <0.7 indicating direct derivation from the upper mantle; while acidic ones with Rb/Sr ratio rice up to 10.7 values suggest the presence oh felsic materials in their source and were derived from sialic crust or indicate crustal contamination.

The Ba/Rb ratio in both the studied basalts and intermediate dykes shows a relatively wide range (6.83-19.44) and generally above the crustal ratio 4.4 of Mason (1966) suggesting that their magma was generated at great depth. While for the acidic dykes the Ba/Rb ratios are far below the crustal average revealing the contribution of sialic crustal material (0.18-4.04)

Y/Nb ratios in the studied dykes exhibits strong variation; for the basic dykes it varies between (1.2-5) with one exceptional value of 0.5; for the intermediate dykes (1.1- 4.5), while for the acidic dykes, these ratio varies between (0.7 - 3.9). Eby (1990) classified the A-type granites into two groups depending on the Y/Nb ratios. He suggested that the first groups with (Y/Nb<1.2) was differentiated from basalitic magma directly derived from (oceanic island basalts) like mantle source. While the second group (Y/Nb = 1.2- 7) exhibits a complex petrogenetic history and may have a significant mantle component, or may be totally of crustal origin. According to this classification, the examined dykes belong to the second group suggesting mantle derivation with crustal contamination.

RADIOACTIVITY

Field radiometric survey was carried out using a calibrated portable gamma ray spectrometer, model Gs-256 (made in Czech), with Nal"Tl- detector, 75X75 mm^2. The uranium and thorium contents of the studied dykes were measured along dyke bodies. The spectrometric data reveals that there is a gradual increase in the eU and eTh contents from basic to intermediate and reach the maximum values in acidic dykes (Table 4). Therefore, the granophyre and rhyolite dykes are the most rock types recommended for uranium and thorium prospection in the studied dykes. The eU and eTh contents and the calculated eTh/eU ratios of 26 samples representing the studied dykes are given in Table (4).

Table 4: Results of Gamma ray spectrometric measurements of the studied dykes

Rock type	S. No.	eU (ppm)	eTh (ppm)	eTh/eU	K%
	1	190	120	0.62	8.0
	2	280	125	0.45	11.0
Rhyolite	3	300	195	065	13.0
	4	260	145	0.56	9.0
	5	200	145	0.72	8.0
Average	246	146.2	0.60	9.8	
	6	90	50	0.55	4.5
	7	140	56	0.40	4.2
Granophyre	8	100	60	0.60	3.0
	9	80	35	0.44	2.2
	10	60	32	0.53	2.0
Average	94	49	0.50	3.2	
	11	5	11	2.2	1.6
Trachyte	12	4	8	2	1.5
	13	3	9	3	1.8
	14	5	12	2.4	1.4
Average	4.25	10	2.4	1.57	
	15	3	12	4	1.5
Trachy-andesite	16	2	10	5	1.4
	17	3	12	4	1.6
	18	4	15	3.75	1.4
Average	3	12.3	4.18	1.5	
	19	2	7	3.5	1.3
Basaltic-andesite	20	3	9	3	1.4
	21	3	8	2.66	1.4
	22	2	10	5	1.5
Average	2.5	8.5	3.54	1.4	
	23	1	2	2	1.0
Basalt	24	2	4	2	1.2
	25	2	5	2.5	1.2
	26	1	3	3	1.1
Average	1.5	3.5	2.38	1.1	

The eU-and eTh-contents in the basalt, basaltic-andesite, trachy-andesite and trachyte dykes range between 1 to 5 ppm and 2 to 15 ppm respectively (Table 4). This indicates homogeneity in the distribution of both eU and eTh due to the narrow range of their distribution. The highest contents are observed in granophyre and rhyolite dykes. The eU-contents in granophyre dyke samples range between 60 to 140 ppm and the eTh- contents range between 32 to 60 ppm. Whereas the rhyolite dyke samples have eU-contents range between 190 to 300 ppm and the eTh- contents range between 120 to 195 ppm (Table 4). These granophyre and rhyolite dykes could be classified as uraniferous rocks as suggested by Darnley (1982) for granites containing uranium at least twice the Clark value (4 ppm). Also the uraniferous rocks are characterized by Zr/Sr ratios greater than 1.65 (Hall and Walsh, 1969).

Normally, thorium is three times as abundant as uranium in igneous rocks (Rogers and Adams, 1969). When this ratio is disturbed, it indicates a depletion or enrichment of uranium while thorium is rather stable for mobilization (Cuney, 1984). The averages of eTh/eU ratios are 0.50 in the granophyre samples while in the rhyolite samples they are 0.60 indicating high contents of uranium relative to thorium (Table 4). This is attributed to the post magmatic processes which cause addition of uranium along fractures and alteration zones.

The relationship between eU and eTh of the studied dykes indicates that the eU increases with increasing eTh from basic to acidic dykes. This is confirmed by the positive relationship observed between eU and eTh (Fig.21). On the other hand, the eTh/eU ratios decrease with increasing eU content from basic to acidic dykes (Fig.22). This confirms the post magmatic enrichment of uranium. The strong positive correlation between eU and Zr reflects the role of magmatic process in the uranium enrichment (Fig.23). In addition the U-enrichment may be related to hydrothermal fluids rich in both U and Zr. However, Krauskopf (1979) stated that the Rb, Y, U and Th ions have large radii and are less extensive to substituting for major ions in common silicate minerals so they segregated and concentrated in late stages of melt differentiation. The observed positive relationship between eU and Rb (Fig. 24) indicates their magma differentiation at shallow depth (Briqueu et al, 1984).

MINERALOGIC INVESTIGATIONS

The high radioactive samples were subjected to heavy liquid separation and picked as individual minerals under the binocular microscope. These minerals were identified by X-ray diffraction (XRD) techniques and confirmed by Environmental Scanning Electron Microscope (ESEM) back-scattered images supported by energy dispersive spectrometer (EDS) unit (model Philips XL 30 ESEM) at

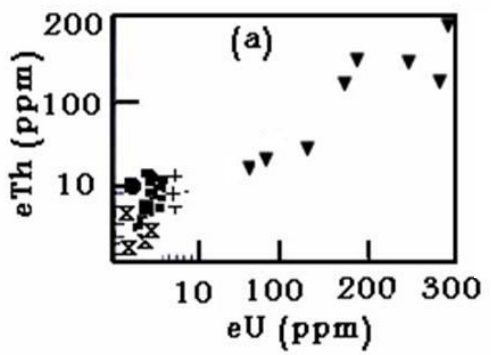

Fig.21: eU variation diagrams (eU-eTh), (Symbols as in Fig.10)

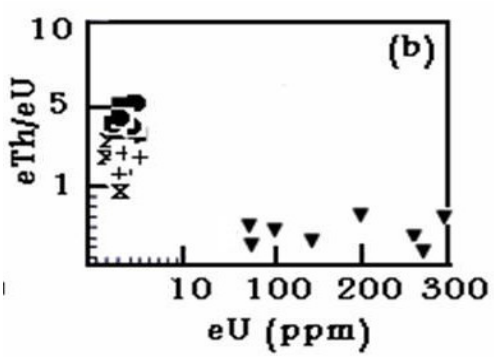

Fig.22: eU variation diagrams (eU-eTh/eU), (Symbols as in Fig.10)

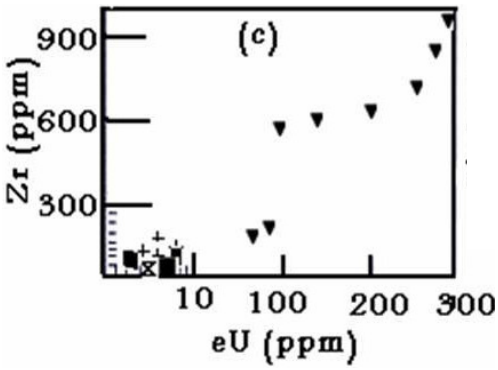

Fig.23: eU variation diagrams (eU-Zr), (Symbols as in Fig.10)

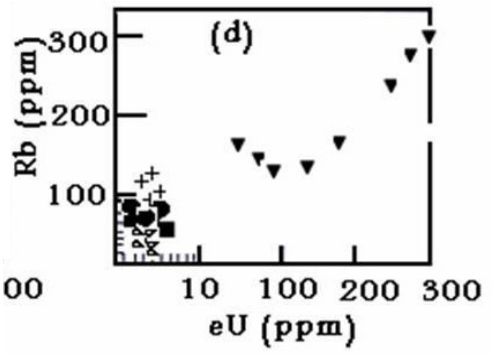

Fig.24: eU variation diagrams (eU-Rb), (Symbols as in Fig.10)

the laboratory of the Nuclear Materials Authority (NMA). The analytical conditions were 25-30 KV accelerating voltages, 1-2 mm beam diameter and 60-120 second counting times. Minimum detectable weight concentration from 0.1 to 1 wt%. Precision is well below 1%, the relative accuracy of quantitative result 2-10% for elements Z>9 (F), and 10-20 % for the light elements B, C, N, O and F. The identified minerals are clarified in the following; secondary U-minerals such as (uranophane and uranothorite) columbite and monazite.

Uranophane ($CaO.2UO_3.2SiO_2.6H_2O$)

Uranophane is secondary uranium mineral in nature and distinguished by its bright colors (canary yellow, lemon and brown of different shades). It is often found as fissure and vein filling. In the studied dykes, uranophane is generally soft (broken easily by a needle); occurring in the form of granular, subhedral to anhedral crystals that sometimes contain black and/or brown inclusions. It exhibits dull or greasy luster and its color varies from canary yellow to lemon. The semiquantitative (EDX) analysis shows its main constituents of the identified minerals by X-ray diffraction (Fig. 25 & 26).

Uranothorite (U, Th) SiO_4

Uranothorite is considered as one of the radioactive mineral that are derived from the

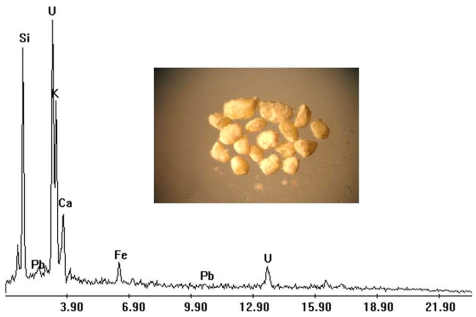

Fig.25: Photomicrograph and back scattered image of uranophane grains

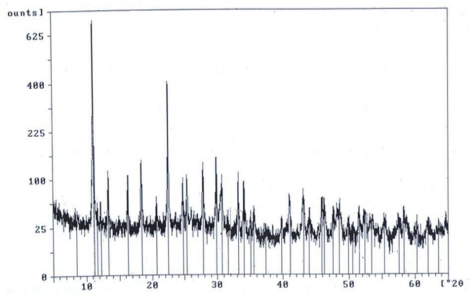

Fig.26: X-Ray diffraction pattern of the uranophane

magma differentiation. Uranothorite may formed by the substitution for Th by U and sometimes rare earth elements and U may reach up to 12% included as UO_2. Uranothorite appears as inclusions in feldspars. This mineral was separated and identified from the non-magnetic fraction under binocular microscope and identified by scanning electron microscope. The semiquantitative (EDX) analysis shows that the major elements in uranothorite are Th (66.83 wt %), Si (11.15 wt %) and U (17.33 wt %). Also, minor amounts of Ca and Fe were reported as substitutions in uranothorite (Fig. 27).

Columbite $(Fe,Mn)(Nb,Ta)_2O_6$

Columbite occurs as black to dark-brown euhedral to subheral grains. It was identified by using scanning electron microscope (ESEM) analyses. The semiquantitative (EDX) analysis shows that the major elements of columbite are Nb (38.44%), Ca (17.76%), Si (6.75%), Ti (5.66%), Pb (3.22%), U (5.46%) and Ta (3.41%) in addition to minor amounts of Th, Fe, Al and K were reported as substitutions. REEs e.g. Ce, Nd and La are also found (Fig. 28).

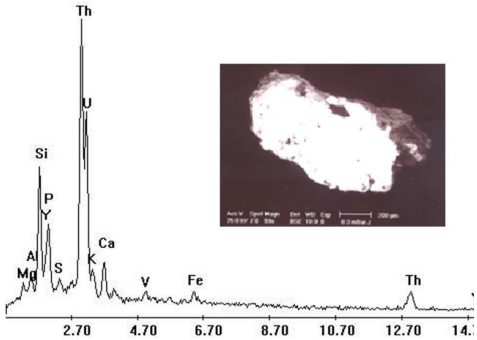

Fig. 27: EDX and back scattered image of uranothorite

Monazite $(Ce,La,Th,\ldots)(PO_4,SiO_4)$

Monazite occurs as a rare earth accessory mineral in granitic rocks, syenites and is found as relatively large crystals in pegmatites (Deer et al., 1992). It is the most common REE-bearing mineral, which has preferential selectivity towards the LREE and is also known as

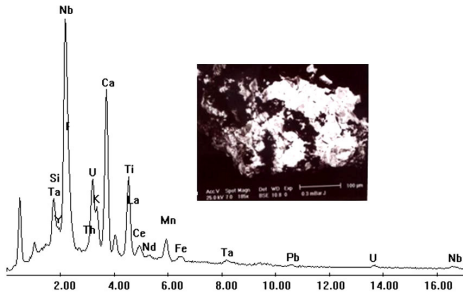

Fig. 28: EDX and back scattered image of columbite.

ultrastable mineral during weathering. The early crystallization of monazite would lead to U enrichment in the residual fluids (Page l, 1982).

The semiquantitative (EDX) analysis by using scanning electron microscope (ESEM) of the studied monazite identified the major elements contains of Ce (33.91 wt %), P (15.86 wt %), La (12.28 wt %), Si (8.93 wt %), Nd (8.02 wt %), Al (4.42 wt %). and appreciable amounts of Th (2.31 wt %), U (0.74 wt %) together with Pr (2.97 wt %), Sm (0.82 wt %), Gd (0.87 wt %), and subordinate amounts of Fe, Ca and K are also found (Fig. 29).

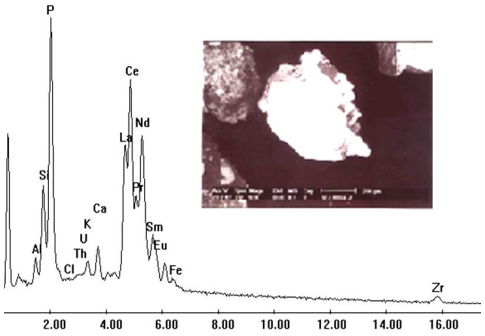

Fig. 29: EDX and back scattered image of monazite

SUMMARY AND DISCUSSION

Field, petrographic, mineralogical and geochemical investigations of the present work indicate that the dyke swarms in Wadi El Akhdar have been classified into acidic, intermediate and basic dykes. The acidic dykes include rhyolite and granophyre. The intermediate dykes comprise trachyte and trachy-andesite. The basic dykes are represented by basalt and basaltic-andesite.

The studied dykes were derived from high calc-alkaline to shoshonite magma. The curvelinear systematic variations for most of the major oxides in the studied dykes could be interpreted as evidence of fractional crystallization. They are peraluminous in nature and classified as hyperaluminous type. They were intruded in synorogenic granodiorites trending in NE-SW and NW-SE. the later trending dykes being younger.

Friz (1991) studying the geochemical characterization of Pan-African dyke swarms in Southern Sinai, reported that at least 3 episodes of lithosphere extinction acting during late Pan-African times in Southern Sinai, were marked by the emplacement of 3 chemically distinguishable dyke swarms. The oldest swarms striking 35°, intruded a calc-alkaline synorogenic granodiorite in Wadi El Sheikh 591±9 Ma ago (Stern and Manton, 1987) these dykes display significant calc-alkaline affinities.

A second generation of 35° trending dykes (L1) was emplaced into the western most extinction of the post orogenic, alkaline Yqma granite within this group few dykes appear to have been contaminated by K, Rb via assimilation of upper crustal components.

The youngest dyke swarm (S2) crosscuts the (S1) dykes at W. El Sheikh at a prevailing strike of 135°. The rocks expose a transitional to mildy alkaline chemistry consistent with a continent tectonic setting. He concluded that the tectonic situation of the Sinai Peninsula developed from an active continental margin to an intra continental setting that was accompanied by a chemical evolution of the subcontinental lithosphere.

Lacumin et,al. 1998, investigated dyke swarms from W. Feiran, W. El Sheikh and Gabal Minadir (Fig.1). These authors reported that the dykes from Gabal Minadir and W. El Sheikh display intermediate and acidic compositions, while those from W. Feiran are mainly basic. They concluded that the studied Sinai dykes can be related to late stages of extensional tectonics of the Pan- African cycle. Comparing the studied dykes from W. El Akhdar and the previously mentioned swarms, one can correlate them with the L1 and S2 phases

of Eriz-Töpfer (1991).

The relationships between mafic and felsic dykes indicate that mafic and felsic magmas co-existed in time as well as in space.

The bimodal basic-acidic dykes of Wadi El Akhdar trending NE-SW probabily belong to the phase of bimodal magmatism resulting from the NW-SE crustal extension (Stern and Manton, 1987). The enigmatic problem is the subsequent intrusion of the intermediate (trachy-andesite and trachyte) dykes trending NW-SE. The bimodality of magma type and the order of emplacement can be best explained by the buoyancy theory of Bonin (1998). According to this theory, to each magma composition corresponds its specific horizon of neutral buoyancy; where it is subsequently converted into a crystal cumulate and residual liquid assemblage. At the deepest level, partial melting produces primary liquids of basaltic composition which can migrate upward. Liquid ascent is favored when pre-existing fractures are stirred up by tectonic disturbances. The primary magma can go directly to the surface and erupte as lava. This may explain the emplacement of the mantle derived basaltic dykes in the studied area. If there is no extensive fracturing, the primary magmas are stored in reservoirs at the mantle-crust boundary. Monzonitic liquids can intern migrate upwards and be stored at the ductile brittle transition of the lower-upper crust boundary.

The major fractionation and assimilation of wall rocks, generating the co-genetic magmatic trends. This may also explain the emplacement of the intermediate dykes trending NW-SE and intersecting the early formed basic-acidic set of dykes. Concering the rhyolitic dykes, similar occurrences were recorded in W. El Sheikh; W. Labowa and W. Feiran by Friz 1987; Lacumin et al., 1998; Stern et al., 1984. Their origination was always a matter of debate. The buoyancy theory used by Bonin, 1998 to explain the formation of rhyolitic dykes in the alkaline ring complexes may explain their presence in the Sinai dyke swarms. They represent the final alkaline liquid trapped in the top of the magma chamber. This alkaline liquid was enriched in radioelements and rare metals responsible for the deposition of these elements in the acidic dykes.

The field radiometric survey and laboratory radiometric measurements indicated that the rhyolite and granophyre dykes are the most important from the radioactive point of view. They are characterized by the presence of uranium and thorium minerals, together with some rare metal minerals. The radioactive minerals are lithologically controlled and also is attributed to post magmatic processes which cause addition of uranium. Uranophane, uranothorite, columbite, zircon and monazite are the main radioactive minerals in the examined acidic dykes.

REFERENCES

Ahmed, A.A., and Youssef, M.M., 1976. Air photo interpretation of dyke swarms in the area around Feiran Oasis, S.W. Sinai, Egypt. Bull. Fac. Sci., Assiut Univ., 5(1), 31-42.

Bonin, B.,1998. Alkaline rocks and geodynamics. J. earth Scin. ,7, 105-118.

Briquieu, I.; Bougnal, T.H., and Joron, J. L.,1984. Quantitfication of Nb, Ta, Ti and V anomalies in magmas associated with subduction zones; Petrogentic implications. Earth Planet. Sci. Lett., 68, 297-308.

Bucanan, M. S., 1982. The geochemistry of some igneous rocks. Geochem and Cosmochem. Acta. 9, 297-308.

Cuney, M. ,1984. Les methods des prospection de l·uranium, Nuclear Energy Agency of the OECD, Paris. 277-292.

Darnely, A. G. ,1982." Hot granite " , Some general remarks . In: uranium in granites (Maurice, Y. T., Ed.). Geol. Surv. Canada. Paper 81-23, p. 1-10.

Deer, W. A.; Howie, R. A., and Zussman, J.,1992. An introduction to the-rock forming minerals. Low- Priced Edition, ELBS, Longman, 528p.

El Mowafy, A.A.,2008. Geology, geochemistry and radioactivity of dykes at Gabal Minadier area, southcentral Sinai, Egypt. Sci. J. Fac. Sci. Minufia Univ., XXII, 147-168.

Friz, A. ,1987. Mineralogie und Geochemie Pan-Afrikanischer Ganggesteine der Suddlicher Sinai_Halbinsel. Dessertation, instate of Mineralogy, Karlsruhe Univ., West Germany.

Friz-Topfer, A.,1991. Geochemical characterization of Pan-African dyke swarms in southern Sinai from continental margin to intaplate magmatism. precambrian Res., 49, 281-300.

Hall, A. , and Walsh, J.N. ,1969. Rapid method for the determination of fluorine in silica rocks and minerals. Anal. Chem. Acta, 45, 341-352.

Irvine, T.N. , and Baragar, W.R.A. ,1971. A Guide to the Chemical Composition of the common volcanic rocks, Can. J. Earth Sci., 8, 523-548.

Krauskopf, K.B.,1979. Introduction to geochemistry. 2nd Ed. McGraw-Hill Book Co. London, 617p.

Lacumin, M.; Marzoli, A.; El-Metwally, A.A., and Piccirillo, M. E.,1998. Neoproterozoic dyke swarms from southern Sinai (Egypt): geochemistry and petrogenetic aspects. J. Afri. Earth Sci., 26 (1),49-64.

Le Maitre, R.W.; Bateman, P.; Dudek, A.; Keller, J.; Lameyre, L.e.; Bass, M.J.; Sabine, P.A.; Schmid, R.; Sorenson, H.; Streckeisen, A.; Woolley, A.R. and Zanettin, B.,1989. A classification of igneous rocks and glossary of terms. Blackwell, Oxford.

Mason, B.,1966. Principles of geochemistry ,3rd edition. John Wiley & Sons, New York, 239p.

Pagel, M.,1982. The mineralogy and geochemistry of uranium and thorium and rare earth elements in two radioactive granites of the Vosages, France. Mineralogical Magazine ,46, 152-173.

Pearce, J.A., and Norry, M.G.,1979. Petrogenetic implications of Ti, Zr, Y and Nb variations in volcanic rocks. Contr. Miner. Petrol., 69, 33-47.

Peccerillo, A., and Taylor, S. R.,1976. Geochemistry of Eocene calc-alkaline rocks from the Kastamonu area, northern Turkey. Contr. Min. Petrol., 58, 63-81.

Philips, 1994. X40 Software for XRF analysis. Software Operation Manual. 425. Nederlandse Philips Bedrijven, Amsterdam.

Rogers, J.J.W., and Adams, J.S.S.,1969. Uranium. In: Handbook of geochemistry (Wedepohl, K.H.,Ed.). New York, Springer-Verlag. 4, 92 B1-92.C10.

Stern, R. J.; Gottfried, D.G., and Hedge, C. E.,1984. Late Precambrian rifting and crustal evolution in the North Eastern Desert of Egypt. Geology, 12, 168-172.

Stern, R. J., and Manton, W. I.,1987. Age of Feiran basement rocks, Sinai: implications for late Precambrian crustal evolution in northern Afro-Arabia. J. geo. Soc. Lond. ,144, 569-575.

Sun, S.S., and Nesbitt, R.W.,1978. Geochemical regularities and genetic significance of ophiolite basalts. Geology, 6, 689-693.

Zalata, A. A.,1988. On the dyke swarms of Wadi El Akhdar area, central Sinai, Egypt. Mans. Sci. Bull. ,15 (2), 245-269.

جيولوجية و جيوكيميائية و إشعاعية حشود القواطع بمنطقة وادى الأخضرجنوب وسط سيناء – مصر

عبد المعز صادق و عبد الهادي عباس

تقع منطقة وادى الأخضربين خطى طول ٤١″ ٣٣′ ٣٣° ـ ٩″ ٣٥′ ٣٣° شرقا ودائرتى عرض ٤٥″ ٤٨′ ٢٨° ـ ٣٠″٥٤′ ٢٨° شمالا وهذه المنطقة مغطاة بالصخور الجرانيتية القديمة والحديثة مقطوعة بمجموعة من الحشود فى اتجاهين مختلفين و ذات نوعيات صخرية مختلفة؛ منها القاعدية ممثلة بالبازلت، والحامضية ممثلة الريوليت والجرانوفير والتراكيت

متخذة إتجاة الشمال الشرقى - الجنوب الغربى وأخيرا القواطع المتوسطة الممثلة بالتراكي أندسيت والأندسيت متخذة إتجاة الشمال الغربى - الجنوب الشرقى.

توصلت الدراسة إلى أن هذة القواطع مشتقة من ماجما كالس قلوية غنية بالبوتاسيوم - عمليات التبلور التمايزى وأنها من النوع الغنى بالألومينا و تكونت تكتونيا داخل الالواح او على حافة القارات. وأشارت الدراسة إلى أن تمعدنات اليورانيوم و الثوريوم محكومة بالتكوين الصخرى وبعد عمليات التى ادت الى اضافة عنصر اليورانيوم وتتواجد بالأخص فى القواطع الحامضية وأن هذة التمعدنات ممثلة بمعادن اليورانوفين واليورانوثوريت والكلومبيت والمونازيت.